applied biosciences

MDPI

Article

Evaluation of Nucleoprotein-Based Multiepitope DNA Vaccine Constructs Against CCHFV: Insights from Immunoinformatics and In Vivo Challenges

Sumeyye Altunok [1,2], Mutlu Erdogan [1,*] and Aykut Ozkul [3,*]

[1] Institute of Biotechnology, Ankara University, 06135 Ankara, Turkey; altunok.1@osu.edu
[2] Department of Neurology, The Ohio State University Wexner Medical Center, Columbus, OH 43210, USA
[3] Virology Department, Faculty of Veterinary Medicine, Ankara University, 06110 Ankara, Turkey
* Correspondence: mutluerdogan@ankara.edu.tr (M.E.); ozkul@ankara.edu.tr (A.O.)

Abstract

Background: Crimean-Congo hemorrhagic fever (CCHF) is a severe tick-borne viral disease with a high fatality rate, and no licensed vaccines are currently available. The nucleoprotein (NP) of the Crimean-Congo hemorrhagic fever virus (CCHFV) plays a critical role in viral replication and immune recognition, making it a promising target for vaccine development. This study aimed to design and evaluate a multiepitope recombinant DNA vaccine targeting the NP of CCHFV. **Methods**: Cytotoxic T lymphocyte (CTL) epitopes from the NP were predicted via immunoinformatics approaches and systematically assessed for antigenicity, allergenicity, toxicity, hydrophobicity, and global population coverage. The selected epitopes were incorporated into four DNA vaccine constructs driven by a cytomegalovirus promoter, adjuvanted with human β-defensin 3 (hBD3), and fused to the reporter protein mRuby3. The constructs were evaluated in vitro using a fluorescent reporter system designed to provide a readout of TCR signaling upon the co-culture of T lymphocytes with differentiated monocytic cells expressing antigens. In vivo immunogenicity and protective efficacy were assessed in BALB/c (exploratory pilot) and IFNAR$^{-/-}$ mice, a highly susceptible model for viral infection. Cytokine responses were measured to assess immunogenicity. **Results**: In vitro assays showed predominantly antigen-independent T-cell activation, suggesting that nonspecific stimulation inherent to the reporter co-culture system likely obscured the detection of antigen-specific TCR signaling. In vivo analyses in BALB/c mice revealed that the constructs elicited only modest systemic cytokine profiles while CCHFV-specific IgG and IFN-γ secretion remained undetectable, indicating that antigen-specific T-cell and antibody responses were limited. In the IFNAR$^{-/-}$ challenge model, several peptide groups achieved significant 2–3 log reductions in tissue viral RNA and infectious titers ($p < 0.05$ vs. sham). However, the observed viral modulations were insufficient to reach the protective threshold and did not translate to a survival benefit (0%). **Conclusion**: Despite a rational in silico foundation, the multiepitope DNA vaccine constructs demonstrated limitations in inducing potent, antigen-specific immunity across both mouse models. The lack of antigen-specific responses indicates limitations in epitope selection, construct design, and delivery strategies, requiring optimization of next-generation epitope-based vaccines. These findings highlight the complexity of translating computational epitope predictions into functional vaccines, and provide benchmark data as a framework to guide future optimizations.

Check for updates

Academic Editor: Francesco Cappello

Received: 5 November 2025
Revised: 10 February 2026
Accepted: 10 March 2026
Published: 1 April 2026

Copyright: © 2026 by the authors. Licensee MDPI, Basel, Switzerland. This article is an open access article distributed under the terms and conditions of the Creative Commons Attribution (CC BY) license.

Keywords: CCHFV; epitope-based vaccine design; DNA vaccine constructs; T-cell response; immunoinformatics; DNA vaccine delivery; murine models; vaccine evaluation

1. Introduction

CCHF is a tick-borne viral disease caused by CCHFV, a member of the Nairoviridae family within the order Bunyavirales. It represents a major public health threat because of its high case fatality rate, wide geographic distribution, and absence of licensed vaccines or specific antiviral therapies. Clinically, the disease often begins with nonspecific symptoms such as fever, fatigue, and myalgia, but a subset of patients rapidly progresses to severe hemorrhage and multiorgan failure [1]. The presence of subclinical and asymptomatic cases further complicates early diagnosis and surveillance, while the heterogeneity in disease outcomes underscores critical gaps in our understanding of CCHF pathogenesis [2–4].

CCHF is transmitted primarily through the bites of infected Hyalomma ticks, whose geographic distribution has expanded as a result of climate change and ecological disruption [5,6]. This expansion has contributed to an increase in reported cases globally, prompting international health authorities to emphasize the need for improved surveillance and preparedness [7]. Beyond vector-borne transmission, infection can occur through direct contact with infected animal tissues or human bodily fluids, particularly in healthcare settings; furthermore, international travel and migration increase the risk of viral introduction into nonendemic regions, increasing the likelihood of outbreaks in both endemic and previously unaffected areas [7–9].

Currently, there is no globally licensed vaccine or specific antiviral treatment for CCHF [9,10]. Management relies mainly on supportive care, whereas ribavirin has been used off-label with inconsistent clinical outcomes [10,11]. The use of the only available vaccine on a limited scale in Bulgaria is hampered by poor immunogenicity, safety concerns, and the requirement for multiple booster doses [12]. These shortcomings highlight the urgent need for the development of safer, more effective, and broadly applicable vaccine candidates [13].

In recent years, due to the challenges associated with traditional vaccine development, including its lengthy process and high risk of failure, the need for innovative approaches has heightened. In this regard, immunoinformatics methods have emerged as effective tools for accelerating vaccine development [14–18]. In parallel to these developments, DNA vaccines offer several theoretical advantages over alternative platforms for CCHFV vaccine development: (i) enhanced safety profile compared to live-attenuated or viral vector approaches, particularly important for BSL-3+ pathogens; (ii) ability to induce both cellular and humoral immune responses through endogenous antigen processing and presentation; (iii) stability at elevated temperatures, crucial for deployment in CCHF-endemic regions with limited cold-chain infrastructure; and (iv) rapid design and manufacturing capabilities for emerging pathogen responses [19–21]. However, DNA vaccines have historically shown lower immunogenicity compared to mRNA or viral vector platforms, necessitating optimization of delivery methods and adjuvant strategies.

The CCHFV nucleoprotein represents a particularly attractive vaccine target due to its high conservation across viral strains and established role in eliciting cellular immune responses [22–25]. Unlike the more variable glycoprotein complex, NP demonstrates >80% amino acid conservation across circulating CCHFV isolates, potentially providing broad cross-strain protection. NP is also increasingly recognized as a primary target for cellular immunity in CCHFV infection. Recovered patients exhibit robust memory T-cell responses directed predominantly toward NP, with significantly lower reactivity observed against the

Gn and Gc glycoproteins [24]. Specifically, while NP contains multiple immunodominant CD8+ T-cell epitopes, glycoproteins have shown limited T-cell triggering, suggesting that NP-specific cellular responses may be critical for viral clearance and recovery. Previous NP-targeted vaccine attempts have yielded inconsistent outcomes; while certain viral replicating particle platforms have demonstrated protection through a combination of cellular and humoral responses, other platforms, such as Modified Vaccinia Virus Ankara, have failed to provide survival benefits despite inducing robust antigen-specific immunity [25]. Such inconsistencies arise largely because antibodies against NP generally lack direct neutralizing activity; however, emerging evidence suggests these antibodies may still contribute to protection through Fc-mediated effector mechanisms. Furthermore, studies on related bunyaviruses have demonstrated that NP-specific CD8+ T-cell responses correlate strongly with viral clearance and survival [26–28]. For CCHFV specifically, NP has been shown to elicit cytotoxic T-lymphocyte activation characterized by robust IL-2 and IFN-γ production [25]. Consequently, while NP is a strong target particularly for T-cell-based vaccine strategies, its use as a standalone antigen reveals a challenge in translating potent immunogenicity into a definitive protective threshold.

Therefore, the aim of this study was to design and evaluate a rationally constructed multiepitope DNA vaccine targeting CCHFV NPs. Using a multistep immunoinformatics pipeline, we identified antigenic, nonallergenic, and nontoxic CTL epitopes across the NP sequence. These epitopes were assembled into a multiepitope DNA construct incorporating an hBD3 adjuvant to increase immunogenicity [29–31]. By combining reverse vaccinology with advanced computational screening tools, our work addresses a critical gap in current vaccine research and provides a framework for the experimental validation and preclinical development of next-generation vaccines against CCHF.

2. Materials and Methods

The reverse vaccinology strategy employed in this study consisted of three consecutive stages: in silico epitope prediction, in vitro validation of antigen constructs, and in vivo immunogenicity testing, and the overall workflow of the study is summarized in Figure 1 with the main steps. This multistage design was intended to provide a systematic progression from computational identification of candidate epitopes to biological assessment in both cell culture and animal models.

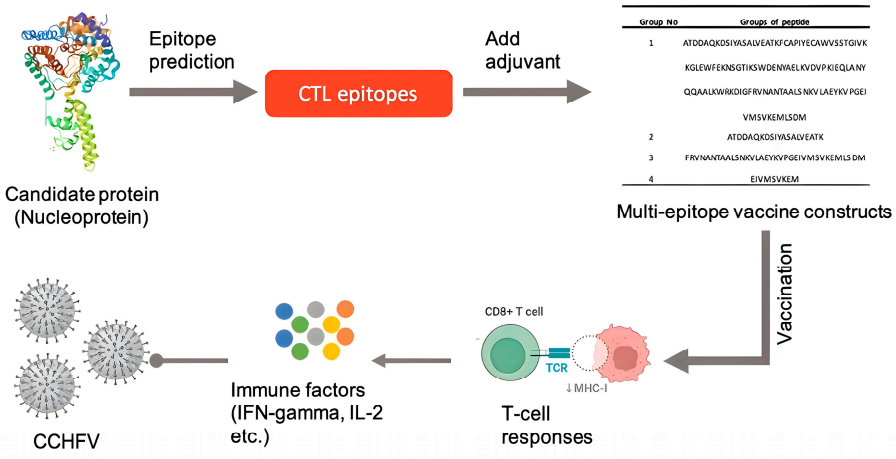


Figure 1. Overall workflow of the study.

2.1. In Silico Analysis

The aim of the in silico stage was to systematically identify CTL epitopes with optimal antigenicity, safety, sequence conservation and population coverage features,

thereby providing rationally selected candidates for experimental validation. The computational pipeline for the development of the multiepitope DNA vaccine was conducted through a hierarchical workflow: (i) large-scale identification of CCHFV-NP sequences retrieved from 221 global strains and isolates; (ii) an epitope pooling strategy that employs three distinct algorithms (IEDB, NetMHC-4.0, and Rankpep) to identify high-affinity MHC-I binders, ensuring a comprehensive capture of potential T-cell targets; (iii) filtering of antigenic epitopes via two distinct antigenicity prediction tools (VaxiJen (https://www.ddg-pharmfac.net/vaxijen/VaxiJen/VaxiJen.html; accessed on 5 November 2025) and Predicted Antigenic Peptides (http://imed.med.ucm.es/Tools/antigenic.pl; accessed on 5 November 2025)); (iv) parallel immunoinformatic analyses of the antigenic epitopes for allergenicity, hydrophobicity, toxicity, world-wide HLA allele population coverage and sequence conservation across the global CCHFV strains to identify potent and safe epitopes; (v) final selection of vaccine candidates prioritizing antigenicity and high sequence conservation.

2.1.1. Protein Sequence Retrieval

The complete NP sequence of the Ank-2 strain (GenBank accession no. MK309333.1; Supplementary Data) was retrieved from the NCBI database. Additional NP sequences from other *Orthonairovirus hemorrhagia* strains and isolates (221 in total) were obtained from NCBI in June 2023 to identify conserved regions (Supplementary Table S1).

2.1.2. CTL Epitope Prediction

CTL epitopes were predicted in parallel via the Immune Epitope Database (IEDB, http://www.iedb.org, accessed on 5 November 2025), NetMHC-4.0 (https://services.healthtech.dtu.dk/services/NetMHC-4.0, accessed on 5 November 2025), and Rankpep (http://imed.med.ucm.es/Tools/rankpep.html, accessed on 5 November 2025). While 9-mer peptides are the canonical major histocompatibility complex class-I (MHC-I) epitope length, peptides of 8–11 amino acids have also been evaluated, as they can effectively bind and elicit T-cell responses [32–34]. To ensure a comprehensive mapping of the CCHFV-NP epitope landscape, MHC-I binding predictions were performed across all available panels of human HLA alleles. For the IEDB analysis, the NetMHCpan 4.1 EL (Eluted Ligand) prediction method was utilized. For NetMHC 4.0, the stringent threshold of $\leq$0.5% (strong binders) was used to filter high-affinity candidates. Rankpep was executed using the binding threshold of 2%. For all prediction tools, default system settings were applied. MHC-I epitopes predicted in parallel were aligned to curate a library of shared candidate sequences, ensuring that the selected peptides were recognized across the three different algorithmic approaches, thus utilizing the strengths of each predictive framework.

2.1.3. Evaluation of the Antigenicity, Allergenicity, Toxicity, and Hydrophobicity of the Peptides

Antigenicity assessment: The antigenicity of the selected MHC-I epitopes was evaluated via VaxiJen 2.0 [35], which predicts antigenicity based on physicochemical properties without requiring sequence alignment. The organism type was set to "virus." For viral proteins, the default threshold was 0.4; however, this threshold would classify the full-length (FL) CCHFV nucleoprotein (NP; antigenicity score: 0.3025) as nonantigenic, contradicting its well-documented immunogenic role in CCHFV infection. To establish a biologically relevant benchmark, the antigenicity score of the native NP (0.3025) was therefore adopted as the baseline reference. Based on this rationale, epitopes with scores exceeding the NP value were considered to possess greater intrinsic antigenic potential than the full-length protein, and thus, the epitopes with an antigenicity score > 0.3025 were selected for further analyses. This approach ensures consistency between computational predictions and

experimental evidence regarding NP immunogenicity. Additional antigenicity validation of the initial epitope library was also performed via the Predicted Antigenic Peptides tool (http://imed.med.ucm.es/Tools/antigenic.pl; accessed on 5 November 2025), which applies the Kolaskar and Tongaonkar methods [36].

Allergenicity prediction: Allergenicity of the selected antigenic CTL epitopes was assessed via three complementary servers—AlgPred 2.0 [37], AllerTOP 2.0 [38,39], and AllerCatPro 2.0 [40]—which employ diverse algorithmic strategies to improve prediction capacity and reliability. For all three tools, the default parameter settings were applied.

Toxicity assessment: Toxicity of the selected antigenic epitopes was predicted via ToxinPred [41], ToxIBTL [42], and CSM-Toxin [43], which estimates toxicity on the basis of peptide sequence features and physicochemical descriptors. For all three tools, the default parameter settings were applied.

Hydrophobicity analysis: Hydrophobicity indices of selected antigenic epitopes were calculated via Peptide v2.0 (http://www.peptide2.com/; accessed on 5 November 2025) using default parameter settings, which provide normalized values relative to glycine (neutral (0) and the most hydrophobic residue (100)).

2.1.4. Population Coverage and Sequence Conservation Analysis

To assess the global relevance of the predicted epitopes, population coverage analysis was performed via the IEDB population coverage tool (http://tools.iedb.org/population/; accessed on 5 November 2025). This analysis did not involve de novo epitope prediction; rather, it assessed the distribution and representativeness of the previously identified epitope–HLA combinations, with a particular focus on human populations within CCHF-endemic regions of Africa, Asia, and Europe. The IEDB Population Coverage analysis was conducted using the "World" population setting to provide a standardized global benchmark. The input data consisted of the specific, pre-selected epitope–MHC-I pairs that emerged from the antigenicity predictions of the initial pool. This ensured that the coverage metrics specifically reflected the frequencies of the HLA alleles targeted by the selected antigenic peptides. In parallel with the population coverage assessment, a sequence conservation analysis was performed to ensure broad-spectrum efficacy. This was achieved by aligning the predicted antigenic peptides against the CCHFV nucleoprotein sequences from the existing viral strain sequences using the multiple sequence alignment tool within the SnapGene Viewer version 8.2.2. This comparative approach enabled the identification of antigenic epitopes that remained invariant across viral strains for a broadly protective vaccine construct capable of circumventing viral mutational escape.

2.2. In Vitro Analysis

2.2.1. Construction of Vectors Expressing Antigens

To evaluate the immunogenicity of the selected candidates across different biological systems, three distinct expression vectors were utilized. Each system was engineered with a specific functional backbone tailored to its downstream application:

(i) pcDNA3.1(+): Utilized as the primary eukaryotic expression vector for in vivo mouse vaccination studies. (ii) Lentiviral Transfer Plasmid (Addgene #135992): Used for generating pseudotyped lentiviral vectors (LV) for the transduction of THP-1 cell lines in T-cell activation studies. (iii) pET-28a(+): Employed for the prokaryotic expression and purification of the CCHFV NP protein used as the coating antigen in ELISA assays.

Following the in silico prioritization, the selected epitope cassettes were integrated into the respective plasmid backbones. To enhance potential T-cell stimulation, a human beta-defensin 3 (hBD3) peptide (45 amino acids) was incorporated as a molecular adjuvant upstream of the epitope sequence, separated by alanine-alanine-tyrosine (AAY) spacers to

ensure efficient proteasomal processing [44]; in the specific case of the lentiviral transfer constructs, the red fluorescent protein mRuby3 was fused to the N-term of the gene cassette to facilitate the detection and quantification of antigen expression (Figure 2). This fluorescent marker was separated from the downstream antigenic sequence during translation by the Porcine teschovirus-1 2A (p2A) peptide. This self-cleaving mechanism ensures that mRuby3 is released as a separate unit, thereby preserving the functional [45]. The expression cassettes were inserted into the vector backbones via seamless ligation cloning extraction (SLiCE).



Figure 2. Gene constructs expressed in THP-1 cells. (**a**) Gene construct used to express antigenic epitopes, (**b**) adjuvant-only negative control gene construct and (**c**) superagonist positive control gene construct. CMV: mammalian promoter; p2A: cleavage sequence; hBD3Adj: adjuvant; L: alanine-alanine-tyrosine linker; NPAg: antigenic epitope; STOP: translation termination signal; MTSAIGILPV: superagonist peptide.

2.2.2. Generation of Lentiviral Vectors (LVs) Pseudotyped with CCHFV Nucleoprotein or Multiepitope Vaccine Constructs

Pseudotyped LVs expressing either the full-length CCHFV NP or the multiepitope vaccine constructs were generated using a triple-transfection system in HEK293 cells. Cells were co-transfected with 10 µg of packaging and envelope plasmids (Addgene #12260 and #8454) together with 15 µg of the engineered #135992 transfer plasmid in 10 cm plates. Antigen-expressing constructs were transfected into HEK293 cells via polyethylenimine (PEI). Viral supernatants were harvested 96 h posttransfection, centrifuged at 500 rpm for 6 min, and passed through a 0.45 µm filter. The filtrate was mixed with a lentiviral concentrator at a 3:1 ratio, incubated overnight at 4 °C with gentle shaking (100 rpm), and subsequently centrifuged to collect precipitated viral particles.

2.2.3. Generation of Cell Lines Expressing Selected Antigen Candidates

All in vitro experiments (which do not involve the infectious CCHFV strain) were conducted under BSL-2 conditions at Ankara University cell culture facilities. THP-1 (ATCC TIB-202) and Jurkat T cells (ATCC TIB-152) were cultured in RPMI-1640 medium supplemented with 10% fetal bovine serum and 1% penicillin–streptomycin, while HEK293 cells were maintained in DMEM supplemented with the same serum and antibiotics. THP-1 cells were differentiated into macrophage-like cells by treatment with 100 ng/mL PMA and 500 ng/mL ionomycin for 48 h. Following differentiation, the cells were washed three times with phosphate-buffered saline (PBS) to eliminate the residual stimulatory effects of PMA/ionomycin. Subsequently, fresh culture medium without PMA/ionomycin was added, and the cells were transferred to new culture plates. To allow stabilization of the macrophage-like phenotype and ensure completion of differentiation, the cells were rested for an additional 24 h prior to co-culture [46,47]. The concentrated viral lentiviral particles were used to transduce THP-1 cells, facilitating the expression of the mRuby3-tagged antigen constructs. This step allowed the THP-1 cells to serve as antigen-presenting platforms, setting the stage for subsequent co-culture assays with Jurkat cells to monitor T-cell activation in response to the expressed epitopes. Expression was confirmed

by fluorescence microscopy, and the resulting antigen-expressing macrophages were co-cultured with Jurkat T cells to assess T-cell responses.

2.2.4. Evaluation of Antigen-Specific T-Cell Responses by ELISpot Assay

ELISpot assays were performed to evaluate T cell–mediated cytokine responses induced by the antigenic constructs. Each experimental condition was tested in three technical replicates. Positive and negative control groups were included on the same plate alongside the experimental groups. Cytokine-producing cells were visualized as spots using bright-field imaging with a Cytation™ 7 Cell Imaging Multi-Mode Reader (BioTek Instruments, Winooski, VT, USA), and spots were automatically identified and quantified using Gen5™ software version 3.11 based on predefined size and intensity thresholds.

2.3. In Vivo Analysis

2.3.1. Ethics Statement

All experimental procedures involving infectious CCHFV were performed at the High-Security Viral Zoonoses Diagnosis, Advanced Research, and Animal Laboratories (BSL-3+ and ABSL-3+) of Ankara University, Faculty of Veterinary Medicine. The mice were housed in HEPA-filtered cages and acclimatized to ABSL-3+ conditions prior to experimentation. The animals were maintained under appropriate housing and feeding conditions throughout the study, and humane euthanasia was applied at the experimental endpoint. The use of animals in this study was approved by the Local Ethics Committee for Animal Experiments of Ankara University (approval no: 18.03.2020/2020-6-54).

2.3.2. Animals and Immunization Protocols

The group sizes were determined in accordance with previous CCHFV vaccine studies and the principles of the 3Rs (replacement, reduction, refinement). IFNAR$^{-/-}$ cohorts (n = 5 per group) were selected to balance ethical considerations with the ability to detect large biological effects on survival, viral load, and cytokine responses, which is consistent with sample sizes commonly employed in high-containment viral challenge studies.

A total of forty female IFNAR$^{-/-}$ mice (6–8 weeks old, 18–22 g; Kobay Deney Hayvanları Laboratuvarı San. ve Tic. A.Ş., Ankara, Turkey) were randomly assigned into eight groups (n = 5 each): four groups received different multiepitope DNA constructs (50 µg/100 µL in nuclease-free water), two groups served as positive controls (MTSAIG-ILPV peptide and full-length NP), and two groups served as negative controls (empty plasmid and sham, i.e., mock-transfected). Vaccines were administered intramuscularly, followed by a booster on day 14. Two weeks after the booster, the mice were challenged intraperitoneally with 200 µL of 10^3 LD_{50} CCHFV-Ank-2. Six days post-challenge, all animals reached euthanasia criteria (the most prominent clinical signs included decreased movement and piloerection). Spleen and liver samples were collected for evaluation. Protective efficacy was assessed by comparing survival, viral load, and cytokine responses across the vaccinated and control groups.

In parallel, BALB/c cohorts (n = 2 per group) were utilized in a pilot capacity to provide an exploratory assessment of cytokine secretion and lymphocyte profiling within an immunocompetent background. This phase was intended to complement the primary assays and to inform a preliminary understanding of the constructs' in vivo visibility and to observe immunological trends. Given the exploratory nature of this survey, these cohorts were analyzed for descriptive patterns rather than formal statistical significance, serving as a foundational baseline for future refinements. Thus, sixteen female BALB/c mice (6–8 weeks old, 22–25 g) were allocated into eight groups (n = 2 each) and immunized according to the same schedule.

2.3.3. Assessment of the Humoral Immune Response in Vaccination Cohorts via Immunoglobulin G (IgG) Responses

SDS-PAGE and Western Blotting

Recombinant NP protein was expressed via the pET-28a-NP plasmid in *Escherichia coli* strain BL21(DE3), after which the cells were lysed with RIPA buffer and purified via Ni-NTA chromatography. The purified fractions were mixed with Laemmli buffer (Bio-Rad Laboratories, Inc., Hercules, CA, USA), boiled at 95 °C for 10 min, and separated by SDS-PAGE. Proteins were transferred to polyvinylidene difluoride microporous membranes via a semidry transfer system, blocked overnight with 5% nonfat milk in phosphate-buffered saline (PBS), and probed with sera from NP-vaccinated mice as primary antibodies. Horseradish peroxidase (HRP)-conjugated anti-mouse IgG was used as the secondary antibody. The signals were visualized via enhanced chemiluminescence and analyzed with the Bio-Rad ChemiDoc imaging platform.

NP-Specific IgG Enzyme-Linked Immunosorbent Assay (ELISA)

To evaluate vaccine-induced antibody responses, an ELISA was performed using both recombinant NP protein and viral lysates as antigens. Vero-E6 cells were infected with CCHFV Ank-2 at a multiplicity of infection (MOI) of 1 and harvested 4 days post-infection. The cell lysates were used as an antigen source, alongside recombinant NPs purified from *E. coli*. High-binding 96-well plates were coated overnight at 4 °C with either recombinant NP (1 μg/well) or standardized amounts of viral lysate (5 μg protein/well). The plates were blocked with 5% milk in PBS and incubated with serum samples collected from each animal (group size: $n = 5$ for IFNAR$^{-/-}$ and $n = 2$ for BALB/c) prior to immunization and two weeks after the first dose. Each serum sample was analyzed in duplicate. After washing, HRP-conjugated goat anti-mouse IgG (1:15,000) was added, and the mixture was incubated for 1 h at room temperature. The reaction was developed using 3,3′,5,5′-tetramethylbenzidine substrate, stopped with 2 M H_2SO_4, and the absorbance was measured at 450 nm. Optical density values were compared between groups via one-way ANOVA with Tukey's post hoc test. The data are presented as the means ± SDs, and $p < 0.05$ was considered statistically significant.

Preparation and Culture of Splenocytes for Cytokine Assays

Splenocytes were harvested from BALB/c mice two weeks after booster immunization and cultured at a density of 1×10^6 cells/well in 6-well plates. After 1 h of incubation, the cells were infected with CCHFV Ank-2 at an MOI of 10 and maintained at 37 °C and 5% CO_2. The supernatants were collected at 24, 48, and 72 h and stored at −80 °C. Th1 and Th2 cytokines (interferon gamma (IFN-γ), interleukin 2 (IL-2), tumor necrosis factor alpha (TNF-α), interleukin 6 (IL-6), interleukin 4 (IL-4), interleukin 10 (IL-10), interleukin 5 (IL-5), and interleukin 13 (IL-13)) were quantified via the LEGENDplex™ Mouse Th1/Th2 Panel (BioLegend, Inc., San Diego, CA, USA) according to the manufacturer's protocol. All samples were run in duplicate, and data were acquired via flow cytometry. Cytokine concentrations were analyzed by one-way ANOVA (or the Kruskal–Wallis test for nonparametric data), followed by appropriate post hoc comparisons. The results are reported as the means ± SDs or medians.

Evaluation of Viral Load in the Lymphoid Organs of Vaccinated Animals

Total RNA was extracted from the spleen and liver tissues of IFNAR$^{-/-}$ mice ($n = 5$ per group) via PureZOL (Bio-Rad, USA). The RNA quality and concentration were determined via NanoDrop spectrophotometry and agarose gel electrophoresis. Viral RNA was quantified via one-step RT-qPCR (Luna Universal Kit, New England Biolabs, Inc.,

Ipswich, MA, USA) on a Rotor-Gene Q system. CCHFV S-segment–specific primers were used (F: 5′-ATGTCCTTCCTCCACTTGAGA-3′, R: 5′-GCTGAGCTGAAGGTTGATGTTC-3′), with GAPDH as an internal control (GAPDH F: 5′-AGGTCGGTGTGAACGGATTTG-3′, R: 5′-TGTAGACCATGTAGTTGAGGTCA-3′). Reactions were performed in technical duplicates with appropriate negative controls. Relative expression levels were calculated via the $2^{-\Delta\Delta Ct}$ method. Relative expression values were compared via unpaired Student's *t* test (two groups) or one-way ANOVA (multiple groups). A p value < 0.05 was considered significant.

Virus Titration in Tissue Homogenates

To evaluate viral infectivity in vivo, spleen and liver tissues collected from IFNAR$^{-/-}$ mice (n = 5 per group, day 6 post-challenge) were homogenized in PBS to obtain 10% (w/v) suspensions. Homogenates were clarified by low-speed centrifugation at 500× g for 5 min at 4 °C and serially diluted 10-fold in duplicate. Each dilution (100 µL) was inoculated onto confluent Vero-E6 cell monolayers in 96-well plates. The cultures were incubated at 37 °C with 5% CO_2 and monitored daily until a complete cytopathic effect was observed in the virus control wells. The infectious titers were calculated as $TCID_{50}$/0.1 mL via the Reed–Muench method [48]. Viral titers were log-transformed prior to statistical analysis and compared across groups via one-way ANOVA.

3. Results

3.1. Using Computational Approaches to Design Multiepitope Peptide Vaccine Candidates

3.1.1. Retrieval of Protein-Encoding Gene Sequences

The NP sequence of CCHFV (482 amino acids, Ank-2 strain; GenBank accession MK309333.1) was retrieved from the NCBI database for subsequent epitope prediction (Supplementary Data). To assess sequence conservation, NP protein sequences from 221 CCHFV isolates representing diverse *Orthonairovirus hemorrhagiae* strains were also obtained (Supplementary Table S1).

3.1.2. Prediction and Selection of Potent Cytotoxic T Lymphocyte Epitopes

IEDB, NetMHC-4.0, and Rankpep platforms were executed in parallel across all available human HLA alleles, considering peptides ranging from 8 to 11 amino acids in length (Supplementary Tables S2–S4). To ensure a high-affinity starting pool, the analysis was restricted to predicted peptides within the percentile rank of <0.51. The prediction platforms collectively identified a total of 280 epitopes within the CCHFV nucleoprotein. To enhance the strength of the selection, a strategy was implemented to identify shared candidate sequences recognized across the three algorithms. By focusing on these overlapping results via identifying consensus sequences, the pipeline ensured that the selected epitopes were supported by multiple computational methodologies. Ultimately, this process yielded a library of 88 unique candidate CTL epitopes, which were subsequently subjected to antigenicity screening to evaluate their capacity to trigger a robust immune response.

3.1.3. Antigenicity, Allergenicity, Toxicity, and Hydrophobicity Prediction of the CTL Peptides

To refine the selection toward epitopes with the highest immunogenic potential, the candidate sequences were evaluated using the VaxiJen v2.0 server (https://www.ddg-pharmfac.net/vaxijen/VaxiJen/VaxiJen.html; accessed on 5 November 2025). While the platform employs a standard threshold of 0.4 for viral proteins, our preliminary analysis revealed that the full-length CCHFV-NP protein, despite its documented clinical immunogenicity, yielded a score of 0.3025. Adhering strictly to the generalized cutoff would have categorized the native protein as non-antigenic, suggesting that the standard cutoff may not

fully reflect the specific immunogenic profile of the *Orthonairovirus* nucleoprotein. To align the computational screening with this established biological activity, the native NP score (0.3025) was adopted as a comparative benchmark. By prioritizing the ones that exceed the baseline of the immunogenic NP, VaxiJen identified 34 antigenic epitopes (Supplementary Table S5). The 88 candidates were also analyzed using the Prediction of Anti-Inflammatory Peptides tool to assess their potential immune signaling direction. A side-by-side comparison with VaxiJen scores served as a supportive reference (Supplementary Table S6).

The 88 candidate epitopes were further characterized through a multi-algorithm safety assessment to evaluate their allergenic and toxic potential (Supplementary Tables S7–S9). To establish a high-confidence safety profile in terms of allergenicity, consensus was sought across the AllerTOP, AllergenFP, and AlgPred platforms. This cross-comparison yielded an overly conservative subset of only three epitopes simultaneously predicted as non-allergenic by all three tools (Supplementary Table S7). Similarly, toxicity was evaluated towards a consensus across ToxinPred, ToxIBTL, and CSM-Toxin, which shared a broader group of 48 non-toxic candidates (Supplementary Table S8). In parallel, a hydrophobicity analysis was conducted via the Peptide 2.0 (https://www.peptide2.com/; accessed on 5 November 2025), which calculates a normalized hydrophobicity index (glycine = 0; most hydrophobic residues = 100). The mean hydrophobicity of the full-length NP (40.46%) was used as a reference, and epitopes with values above this threshold were classified as hydrophobic (Supplementary Table S9).

Only three epitopes (DMIRRRNLIL, RIYMHPAVL, and SVKEMLSDM) fulfilled the strict consensus criteria for both non-allergenicity, non-toxicity, and hydrophobicity. Relying solely on this limited subset posed a risk to the vaccine's overall immunogenic spectrum and coverage. To ensure that potentially relevant epitopes were not overlooked, particularly those conserved across viral strains, all peptides classified as antigenic were retained for subsequent analyses.

The representative antigenic epitopes and their predicted properties are summarized in Table 1. The candidates possess a degree of synergy across the different platforms; for instance, the epitope ASALVEATK displayed an ideal profile, combining high immunogenicity with unanimous non-allergenic and non-toxic predictions. For several other high-priority candidates, such as EIVMSVKEM and TAALSNKVL, the selection was supported by a strong alignment between antigenic potential and a non-toxic classification across the majority of the toxicity platforms. While allergenicity tools occasionally provided varied perspectives, the emphasis was placed on candidates that demonstrated a reliable consensus in their primary immunogenicity and safety scores. This balanced approach ensured that the final library was composed of epitopes with favorable overall profiles, effectively utilizing the complementary strengths of each tool.

3.1.4. Theoretical Population Coverage and Alignment Analysis

To determine the global applicability of the predicted targets, the initial pool of 88 candidate CTL epitopes was subjected to a conservation analysis against the dataset of available CCHFV NP sequences from the global isolates and strains. This analysis allowed for the identification of how frequently each peptide was preserved across circulating CCHFV strains and isolates. Thus, 13 epitopes of the 88 candidates (14.8%) demonstrated a high conservation over 75% and persistently preserved across diverse geographic strains (Supplementary Figure S1). By prioritizing these conserved regions, the search space was effectively focused on the sequences that represent persistent features of the viral proteome, thereby reducing the risk of immune escape.

Table 1. Properties of the representative selected CTL peptides.

Epitope	HLA Types	Immunogenicity Score	Antigenicity	Toxicity	Allergenicity	Length
ASALVEATK	HLA-A*11:01 HLA-A*30:01 HLA-A*68:01 HLA-A*74:01	0.785538 [1]/55.34 [2] 0.339134 [1] 0.505761 [1] 0.140242 [1]	Yes	No †	No	10
EIVMSVKEM	HLA-A*0201 HLA-A*25:01 HLA-A*26:01	66.0 [3] 0.304987 [1]/1911.55 [2] 0.637006 [2]/326.49 [2]	Yes	No †	Yes	9
Epitope	**HLA Types**	**Immunogenicity Score**	**Antigenicity**	**Toxicity**	**Allergenicity**	**Length**
TAALSNKVL	HLA-B*35:03 HLA-C*03:03 HLA-C*03:04 HLA-C*16:01	0.188568 [1] 0.753266 [1]/141.12 [2] 0. 753266 [1] 0.657969 [1]	Yes	No †	Yes	9

Footnotes: † indicates that 2 of the 3 tools used for toxicity produced the same results. Immunogenicity scores of [1] IEDB, [2] NetMHC 4.0, and [3] Rankpep.

To further characterize the human relevance of the identified targets, the 88 consensus epitopes were evaluated using the IEDB Population Coverage tool (Supplementary Table S10). By matching the associated HLA-binding profiles of these sequences to global allele frequencies, we assessed their potential to elicit an immune response across a worldwide population. Within this broader immunological landscape, the 13 epitopes previously identified for their high sequence conservation were examined to determine their specific contribution to the vaccine's anticipated global breadth (Supplementary Figure S1). Population coverage analysis was performed via the IEDB Population Coverage tool, which estimates the probability of individuals responding to a given set of peptides based on the distribution of their corresponding HLA alleles. For each of the predicted epitopes, the associated HLA types were matched to their global allele frequencies by selecting the "World" population option, thereby accounting for the worldwide distribution of HLA alleles. The majority of epitopes presented global coverage values below 50%, with most clustering within the 20–40% range. Although these values may appear modest, they reflect the restricted distribution of certain HLA alleles at the global level and do not preclude the biological relevance of the corresponding epitopes.

Our computational assessment concluded with the selection of 13 epitopes intended to serve as the set for experimental investigation. Rather than a linear immunoinformatic reduction based on individual scores, this group was curated primarily by their high evolutionary conservation (>75% persistence across the global CCHFV landscape), which encompasses a variety of immunogenic and safety profiles (Supplementary Table S11). This selection prioritized a strategic focus on sequences that remain preserved despite the virus's extensive genetic heterogeneity and its circulation across disparate geographical lineages from Sub-Saharan Africa and the Middle East to South-Eastern Europe and Western Asia. The rationale for this conservation-oriented focus was further reinforced by the inherent nuances among immunoinformatic platforms, where different algorithms occasionally provided varying outputs on the same candidate sequences. To balance these predictive variabilities, high conservation was utilized as a consistent thread to navigate the diverse landscape of in silico outputs. By assembling a library that encompasses a spectrum of predicted immunogenic profiles, essentially maintaining a high sequence conservation, this study aimed to explore whether the evolutionary persistence of these segments would align with measurable biological engagement.

A comprehensive summary of the sequential immunoinformatics workflow, including the specific software tools, filtering thresholds, and the strategic selection logic for the final 13 conserved epitopes, is provided in Supplementary (Supplementary Table S12).

3.2. Vaccine Design

For the design of the CCHFV vaccine candidates, thirteen prioritized CTL epitopes were grouped into five multiepitope constructs (Table 2). These epitopes were strategically clustered to preserve antigenic continuity along the CCHFV-NP protein. By maintaining the original sequence architecture where predicted epitopes overlapped or nested, we ensured the structural integrity of the primary sequence was not disrupted. This grouping strategy reflects a rational design approach aimed at maximizing immunogenic potential without excluding biologically relevant sequences. For experimental benchmarking, the design included two positive controls: the full-length CCHFV-NP (Ank-2 strain) and a construct encoding the MTSAIGILPV superagonist peptide, a modified influenza M1 epitope utilized to establish a threshold for $CD8^+$ T-cell activation and IFN-γ production [49] (Figure 2).

Table 2. Peptide, negative, and positive groups evaluated for T-cell responses.

Group No	Groups of Peptide or Controls
1	ATDDAQKDSIYASALVEATKFCAPIYECAWVSSTGIVKKGLEWFEKNSGTIKSWDEYAELKVDV PKIEQLANYQQAALKWRKDIGFRVNANTAALSNKVLAEYKVPGEIVMSVKEMLSDM (Peptide group 1)
2	ATDDAQKDSIYASALVEATK (Peptide group 2)
3	FRVNANTAALSNKVLAEYKVPGEIVMSVKEMLSDM (Peptide group 3)
4	EIVMSVKEM (Peptide group 4)
5	MTSAIGILPV peptide (positive control)
6	Full-length NP (Ank-2) (positive control)
7	Empty vector (negative control)
8	Sham-vaccinated (negative control)

Across all expression platforms (pcDNA3.1(+), pET-28a and #135992), the antimicrobial peptide hBD3 was incorporated as a molecular adjuvant to enhance immunogenicity and followed by an alanine-alanine-tyrosine (AAY) spacer that is linked to the relevant epitopes. However, the constructs specifically engineered into the #135992 lentiviral transfer backbone featured an N-terminal fusion of the fluorescent protein mRuby3 to facilitate the quantification of transduction efficiency in THP-1 cells used in vitro co-culture assays (Figure 2). To produce the functional lentiviral particles, this engineered transfer plasmid was co-transfected into HEK293 cells along with the Addgene gag-pol (#12260) and envelope (#8454) packaging vectors [50]. This lentiviral vector system has been previously validated and widely applied in our laboratory for a range of applications.

To evaluate the baseline cellular activation induced by the adjuvant alone, a dedicated hBD3-only control lacking antigenic epitopes was generated; for in vitro assays, this adjuvant-only control contained mRuby3 at the N-terminus (Figure 2). Additional negative controls used across all platforms are the empty plasmid vector and sham vaccination.

3.3. In Vitro T-Cell Activation Assays Revealed Predominantly Antigen-Independent Responses

To explore antigen-specific T-cell activation under controlled in vitro conditions, an experimental platform was established by co-culturing Nuclear Factor kappa-light-chain-enhancer of activated B cells (NF-κB) reporter Jurkat cells with antigen-expressing THP-1

cells. Lentiviral constructs were first generated in HEK293 cells (Figure 3a) and used to transduce THP-1 cells, where successful transduction was verified by mRuby3 fluorescence (Figure 3b). THP-1 cells were then co-cultured with NF-κB reporter Jurkat cells to monitor GFP expression as a readout of TCR signaling (Figure 3c).

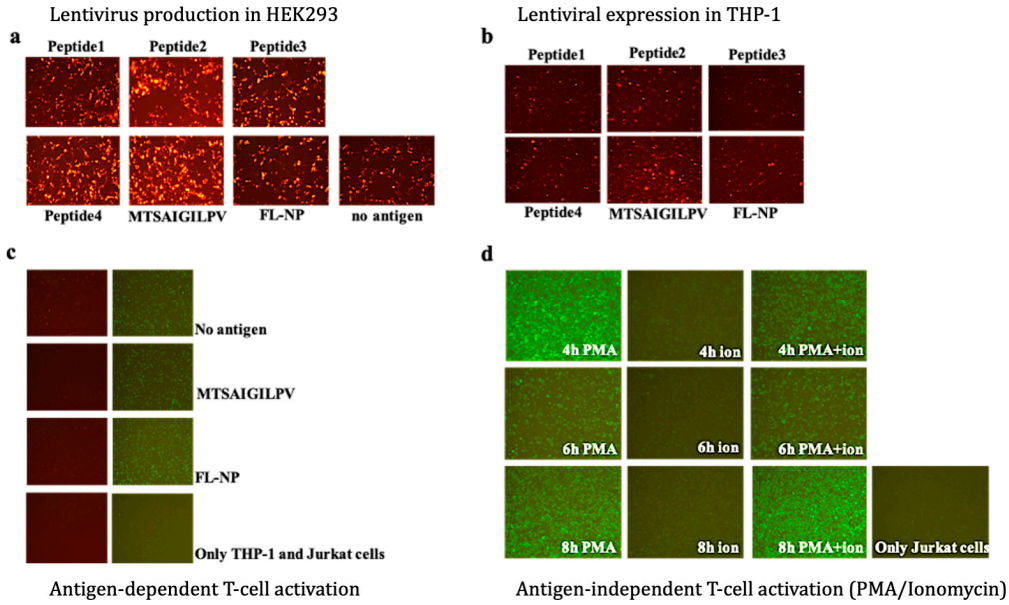


Figure 3. In vitro co-culture system designed for evaluating T-cell responses. (**a**) Lentivirus production in HEK293 cells. (**b**) Lentiviral expression in THP-1 cells. (**c**) Co-culture of antigen-expressing THP-1 cells and Jurkat$^{NF\text{-}kB}$ cells. (**d**) PMA/ionomycin concentrations used for THP-1 differentiation triggered potent, antigen-independent activation of Jurkat$^{NF\text{-}kB}$ cells. A time-dependent increase in GFP fluorescence was observed at 4, 6, and 8 h.

Prior to co-culture, THP-1 cells were differentiated into macrophage-like cells using PMA and ionomycin to ensure the expression of the necessary machinery for antigen presentation and co-stimulation. However, the differentiated state of these cells triggered robust GFP expression in the Jurkat reporter cells independent of the presence of CCHFV antigens (Figure 3c). While preliminary controls confirmed that direct Jurkat exposure to PMA can induce such signaling (Figure 3d), the thorough washing protocols employed post-differentiation of THP-1 suggest that the observed nonspecific activation was likely driven by the inherent stimulatory profile of the macrophage-like phenotype. Accordingly, co-cultures using naive, undifferentiated THP-1 cells did not elicit any detectable signal in the Jurkat reporter (Figure 3c, bottom panel), indicating that the nonspecific signal was likely a consequence of the myeloid maturation required for antigen presentation. Furthermore, extended 48 h co-culture periods resulted in widespread, antigen-independent reporter activity. These findings underscore the limitations of this specific assay system, as the high baseline signaling generated by the differentiated myeloid cells masked the fine-scale, antigen-specific TCR signatures.

Flow cytometry and IFN-γ ELISpot assays were employed to further characterize the T-cell responses, providing an additional layer of resolution to the co-culture findings. Interestingly, while the differentiated THP-1 phenotype induced strong NF-κB-driven GFP signaling in Jurkat cells, this did not translate into significant IFN-γ secretion, which remained comparable to antigen-negative controls (Figure 4a). This discrepancy likely indicates an inherent limitation to the Jurkat cell line, which, while highly sensitive as a transcriptional reporter for early TCR signaling, exhibits a high threshold for the secretion of mature effector cytokines. Similarly, in the pilot study using the immunized BALB/c mice, the peptide-based constructs did not elicit detectable IFN-γ responses above the

background level (Figure 4b). Microscopic evaluation further confirmed the absence of robust IFN-γ spot formation across peptide groups (Figure 4c). The absence of measurable responses across both in vitro and in vivo models suggests that the current design of the multi-epitope vaccine constructs may not provide sufficient antigenic stimulus to overcome the natural activation thresholds of the Jurkat and BALB/c T-cell frameworks.

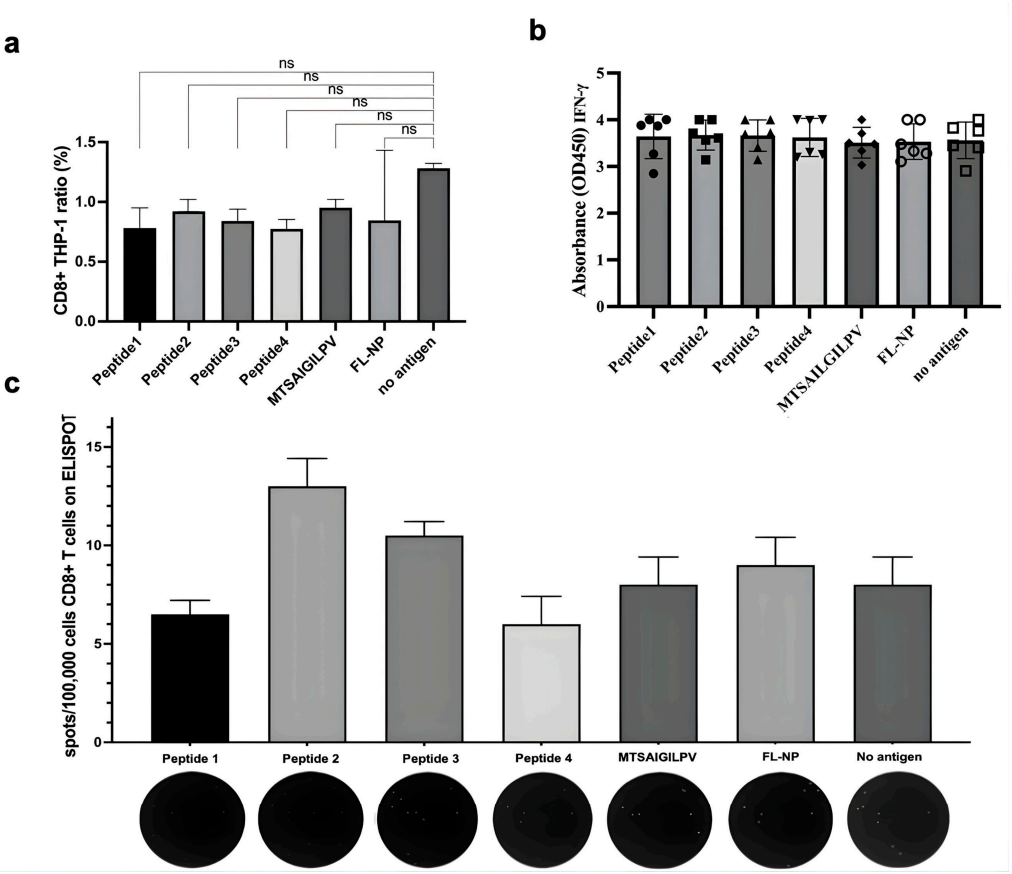


Figure 4. T-cell responses assessed by flow cytometry and the IFN-γ ELISpot. (**a**) Flow cytometric analysis of the Jurkat reporter system following co-culture with antigen-expressing THP-1 cells. Data represent the percentage of Jurkat cells expressing the NF-κB-driven reporter protein. No significant induction was observed in peptide-expressing groups compared to the no-antigen control (ns: not significant; one-way ANOVA). (**b**) Exploratory assessment of bulk IFN-γ secretion (OD450) via ELISA in BALB/c splenocyte supernatants following peptide stimulation. (**c**) Frequency of individual IFN-γ secreting splenocytes isolated from immunized BALB/c mice quantified by ELISpot, expressed as spot-forming cells (SFCs) per 100,000 $CD8^+$ T cells. Error bars represent mean ± SD. For (**a**), significance was determined via one-way ANOVA. For the BALB/c pilot study (**b**,**c**), data are presented as exploratory and descriptive observations due to the small cohort size of $n = 2$.

3.4. Immunizations with Peptide Cohorts, Including FL-NPs, Did Not Elicit CCHFV-Specific IgG Responses

To explore the antigen-specific humoral response in an immunocompetent background, serum samples from BALB/c mice ($n = 2$ per group) were screened for anti-CCHFV IgG antibodies via an in-house ELISA (Supplementary Figure S2). Consistent with the pilot nature of this cohort, these data were not intended for formal statistical evaluation but rather served as preliminary descriptive observations. Endpoint titration curves showed a dilution-dependent decrease in the OD450 values across all the groups (Figure 5). A cutoff value of 0.219, calculated as the mean plus two standard deviations of the sham-vaccinated group, was applied to define seropositivity [51]. None of the peptide- or NP-immunized groups exceeded this threshold at any dilution, suggesting that under the present con-

ditions, the tested vaccine constructs did not generate a detectable IgG response. These findings were considered exploratory and complementary to the IFNAR$^{-/-}$ model analyses, guiding the design of subsequent studies.

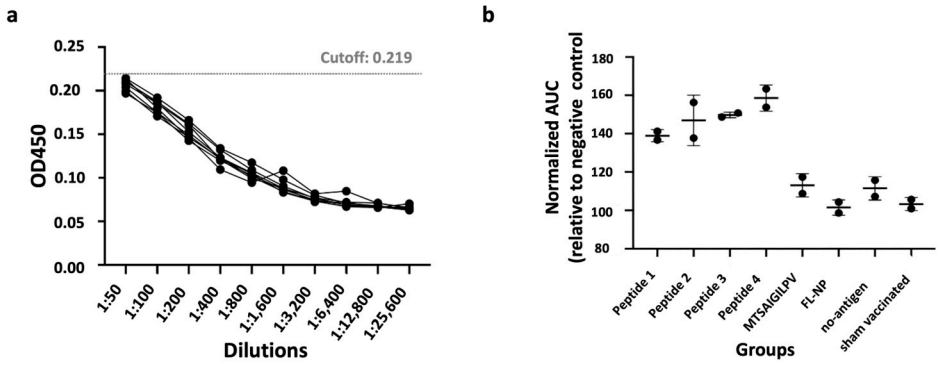


Figure 5. Evaluation of CCHFV-specific IgG levels via ELISA. Serum samples from BALB/c mice were tested at serial dilutions. (**a**) OD450 obtained across serial serum dilutions for the tested groups. Each solid line represents an individual serum sample from the corresponding immunized group. The dashed line indicates the cutoff value (OD450 = 0.219), calculated as the mean plus two standard deviations of the sham-vaccinated control group. (**b**) Normalized area under the curve (AUC) values for each experimental group, expressed relative to the negative control.

3.5. The Two-Dose Prime-Boost Regimen Reduced CCHFV Viremia

To assess the effects of peptide-based vaccine candidates and control formulations on viral replication after CCHFV challenge, viral RNA levels were quantified in the spleen and liver tissues of IFNAR$^{-/-}$ mice via qPCR. Quantitative PCR analysis of viral RNA from lymphoid organs (liver and spleen) was performed on samples collected from animals that succumbed to the disease within six days post-infection. Both the peptide-vaccinated groups and the positive control groups (MTSAIGILPV peptide and FL-NP) exhibited statistically significant reductions in viral RNA load compared to the sham-vaccinated group (Figure 6a,b). This log-scale decline was illustrated by the shifts in the amplification cycles, as shown in the raw Ct values (Supplementary Tables S13 and S14) and the corresponding qPCR amplification curves (Supplementary Figure S3). However, these reductions in viral load did not correspond to improved survival outcomes (Figure 7). Animals in the peptide and positive control groups presented mortality patterns similar to those of the negative controls, despite lower viral RNA levels in lymphoid tissues.

This divergence suggests that the observed reduction in viral burden was likely subthreshold, failing to reach the level of control necessary to prevent the rapid systemic pathogenesis characteristic of CCHFV in the highly sensitive IFNAR$^{-/-}$ model. Furthermore, as survival was monitored for 6 days and viral load was measured at a single time point, these findings provide a snapshot of the peak infection period but do not fully capture the disease kinetics or potential immunological correlates of protection that might emerge in a less acute model.

Although sham controls were included, the absence of an irrelevant antigen control limits interpretation, as it remains uncertain whether the observed reductions were strictly antigen specific. Thus, it cannot be definitively distinguished between antigen-specific immunity and nonspecific innate activation potentially triggered by the delivery platform or the peptides themselves. Nevertheless, the log-scale decline in viral RNA suggests that the constructs exerted measurable biological activity, even though not confirmed as antigen-specific prophylactic effect on viral replication, which emphasizes the need for future studies to incorporate additional time-point analyses, larger cohort sizes, and specificity controls to fully disentangle the mechanisms of protection.

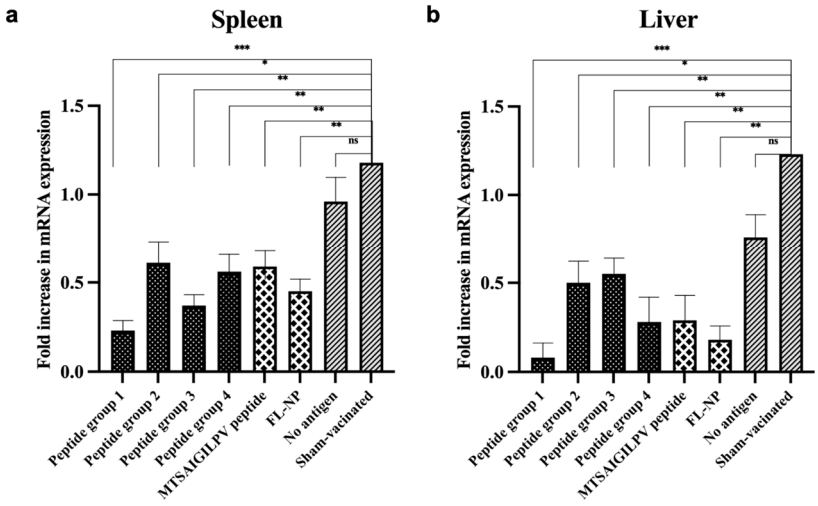


Figure 6. Quantitative PCR analysis of CCHFV-S segment RNA levels in (**a**) the spleen and (**b**) liver tissues of mice challenged with the virus following vaccination. Statistical comparisons were performed relative to the sham-vaccinated group. * $p < 0.05$; ** $p < 0.01$; *** $p < 0.001$; ns, not significant.

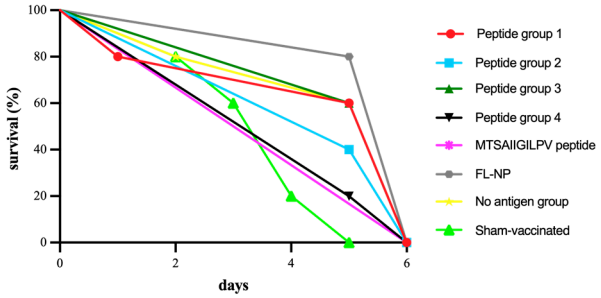


Figure 7. Survival analysis of mice following CCHFV challenge. The animals were monitored for 6 days post-infection, two weeks after the second immunization. Peptide groups received peptide-based vaccine formulations, whereas MTSAIGILPV peptide and full-length NP (FL-NP) constructs served as positive controls. The negative controls consisted of no-antigen and sham-vaccinated groups. Survival percentages are shown over time.

3.6. The Prime-Boost Vaccination Regimen Failed to Confer Protection Against the Disease

Viral infectivity and protective efficacy of the vaccine candidates were assessed by performing a lethal challenge assay. IFNAR$^{-/-}$ mice were challenged with 100 LD_{50} of the Ank-2 strain following a two-dose immunization regimen and monitored daily for morbidity (weight loss) and mortality. On day six post-challenge, liver and spleen tissues were harvested and homogenized to quantify infectious viral titers. Viral infectivity was determined using the Tissue Culture Infective Dose 50% ($TCID_{50}$) assay on Vero cell monolayers. Briefly, tissue homogenates were prepared in serial ten-fold dilutions and cultured in 96-well plates in duplicate. The cultures were incubated at 37 °C until the virus-only controls exhibited 100% cytopathic effect (CPE), at which point titers were calculated using the Reed and Muench method.

Several peptide-based DNA vaccine groups (excluding peptide group 1) demonstrated measurable reduction in viral replication in target tissues with titers ranging from $10^{2.34}$ to $10^{2.5}$ $TCID_{50}$/0.1 mL. This corresponded to an approximate 2-log reduction compared with that of the full-length NP group ($10^{4.4}$ $TCID_{50}$/0.1 mL) and the sham control ($10^{3.8}$ $TCID_{50}$/0.1 mL). Notably, peptide group 4 and the MTSAIGILPV construct exhibited the most pronounced reductions.

Unexpectedly, the viral titers in the full-length NP group were greater than those in the sham group. Potential explanations include (i) inefficient antigen expression or

presentation of the NP, (ii) variability in sampling due to early mortality in some animals, (iii) possible immunomodulatory effect of the NP, as described for certain viral proteins, or (iv) partial innate immune activation by the sham preparation.

Despite measurable reductions in tissue viral titers for the selected peptide groups, these differences did not translate into improved survival outcomes. Nevertheless, the magnitude of the log-scale reductions is biologically meaningful and indicates that some peptide constructs can affect viral replication. Future work with optimized delivery systems, larger cohort sizes and appropriate irrelevant antigen controls is required to determine whether these reductions can be harnessed for protective immunity.

3.7. T Cells Did Not Produce Th1/Th2 Cytokines in Response to CCHFV

Cytokine responses were assessed in splenocyte culture supernatants from BALB/c mice immunized with peptide-based vaccine candidates to evaluate the polarization of the T-cell response following in vitro stimulation with the CCHFV Ank-2 strain. Measurements were performed at 24, 48, and 72 h post-stimulation.

IFN-γ levels remained below the detection limit in all groups and time points, indicating the absence of a measurable Th1-type response (Figure 8a). TNF-α showed a modest time-dependent increase, particularly at 72 h, in the FL-NP, MTSAIGILPV, and control groups, although the values remained <1000 pg/mL (Figure 8b). The IL-2 levels were consistently low, with only a minor increase at 72 h in the FL-NP and MTSAIGILPV peptide groups, but the concentrations did not exceed 500 pg/mL (Figure 8c). Similarly, IL-6 secretion increased over time in the same groups, most noticeably at 72 h (Figure 8d). The similarity between the peptide-immunized and sham groups suggests that the observed cytokine secretion may reflect non-specific background activation rather than antigen-specific T-cell polarization.

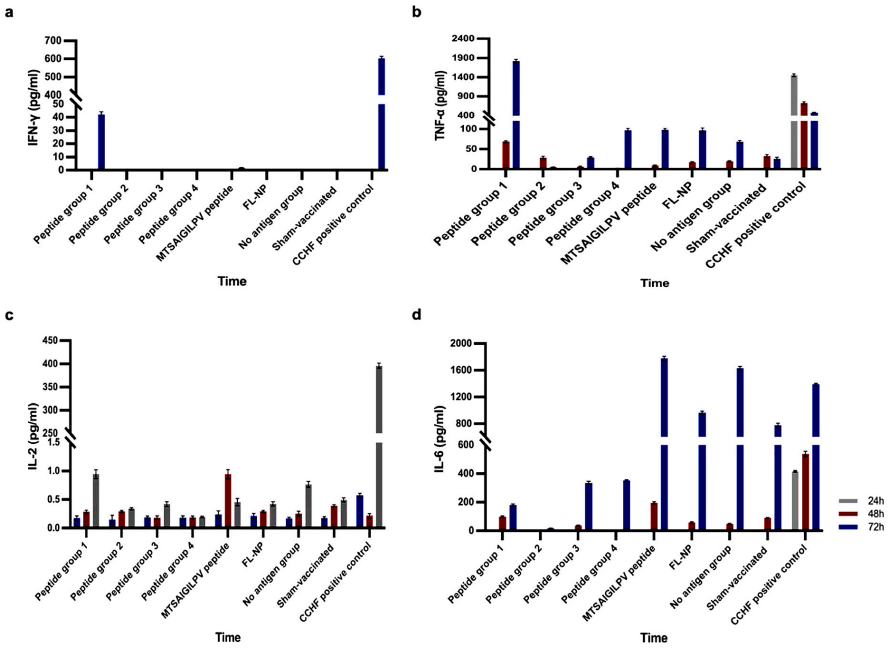


Figure 8. Cytokine responses of splenocytes from vaccinated BALB/c mice after ex vivo restimulation with CCHFV. Splenocytes were isolated from immunized mice and restimulated in vitro with CCHFV-Ank-2, and cytokine levels were measured in culture supernatants. Panels show (**a**) IFN-γ, (**b**) IL-2, (**c**) TNF-α, and (**d**) IL-6. The data represent the means ± SDs.

These limited cytokine differences that contrasted with the significant 2-log reduction in infectious viral titers observed in the IFNAR$^{-/-}$ model necessitate a tempered interpre-

tation of the results. The chosen endpoint for viral quantification (day 6 post-challenge) was specifically selected to capture peak viral replication within the narrow window of this lethal model; however, the lack of a corresponding survival benefit suggests that these biological gains did not reach the clinical threshold required for recovery.

A major confounding factor in interpreting these results is the role of hBD3, which may function as an active immunological driver rather than a passive enhancer. The observation of comparable cytokine patterns in control groups suggests that hBD3-induced signaling could potentially contribute to the baseline cytokine levels observed across all cohorts. This inherent activity of the adjuvant may also mask weaker, epitope-driven responses, complicating the differentiation between adjuvant-mediated innate stimulation and antigen-specific adaptive immunity.

Consequently, while the reduction in viral burden indicates a biological activity relevant to the constructs, the lack of robust cytokine differentiation and the absence of irrelevant antigen control underscore the need for more refined experimental designs. Furthermore, the inclusion of cellular proliferation assays in future studies may offer a more sensitive measure of T-cell expansion, potentially capturing subtle antigen-specific responses that were not evident through cytokine profiling alone. Future work should consider extended time points and larger cohort sizes to effectively decouple adjuvant-driven activation from epitope-specific immunity, ensuring that the virological impact can be clearly linked to a defined immune mechanism.

4. Discussion

The re-emergence of infectious diseases and the increasing frequency of new infections have underscored the urgent need for more effective and cost-efficient therapeutic strategies [52,53]. While traditional platforms offer robust immunity, bioinformatics-driven multiepitope vaccines have emerged as promising alternatives due to their safety and targeted nature [54–56]. This study pursued two primary objectives: the in silico design of a multiepitope vaccine targeting the highly conserved CCHFV nucleoprotein (NP), and the subsequent experimental validation of these candidates. However, our findings reveal significant discrepancies shifting from computational predictions to biological outcomes, providing a transparent benchmark for the challenges of translating immunoinformatics into functional immunity.

4.1. Mechanistic Analysis of Experimental Challenges

The failure to achieve robust antigen-specific immune responses can be attributed to several interconnected factors operating at different levels of the vaccine-host interaction. Antigen-related factors and delivery platform limitations must be distinguished:

Antigen Processing and Presentation Constraints: Unlike direct peptide pulsing, our DNA-encoded epitopes require successful transcription, translation, proteasomal processing, and MHC-I loading, each step representing a potential bottleneck. In a multiepitope string, the proteasome must cut the string at exactly the right spots. With the flanking sequences that are not ideal, the epitopes may be destroyed or never be released. It is possible that the multi-epitope string produced a long chain of proteins that the cell could not chop into the correct 9-mer pieces, meaning they may have never reached the ER to be loaded onto MHC-I. On the one hand, the observation that the MTSAIGILPV superagonist peptide failed to elicit expected responses indicates a complication other than antigen-specific limitations. MTSAIGILPV has been shown to be strictly affine to HLA-A*02:01 [50], thus its failure may be explained by the absence of this specific MHC-I allele in the experimental models used. Alternatively, it is likely that even if the appropriate allele was present, the peptide was not efficiently liberated from the multiepitope polyprotein and failed to reach

the threshold concentration, because the robust expansion for MTSAIGILPV is typically seen over a 14–28-day window. In the specific case of the THP-1/Jurkat co-coculture reporter system, the lentiviral-mediated delivery system may have suffered from suboptimal antigen presentation levels or inappropriate subcellular localization.

Immunodominance and Epitope Competition: The multiepitope design, while theoretically advantageous, may have introduced competitive inhibition between epitopes for MHC-I binding sites or proteasomal processing [15,44,57]. Individual epitopes that showed promise in computational analysis may have been overshadowed by more dominant sequences within the construct, or processed into suboptimal fragments that differ from the predicted epitopes. Despite advances, epitope-based vaccine design continues to encounter challenges, including prediction errors, limited consideration of immune tolerance, and host variability [57]. Progress in artificial intelligence and multi-omics integration could narrow the gap between computational prediction and experimental validation.

Delivery Platform Limitations: The choice of DNA vaccine platform, while offering safety advantages, may have constrained immunogenicity compared to more potent delivery systems. DNA vaccines typically require optimization strategies such as electroporation, gene gun delivery, or heterologous prime-boost regimens to achieve robust immune responses [19,21,58]. Our intramuscular injection approach, while standard, may have been insufficient to drive the level of antigen expression needed for effective T-cell priming. The intramuscular route might have yielded modest immunogenicity because muscle tissue is typically APC-poor, with antigen expression mostly restricted to myocytes that cannot effectively prime naïve T-cells, which creates an immunological bottleneck. As a consequence, intramuscular delivery relies on the inefficient recruitment of circulating dendritic cells; thus, future designs should target more immunologically active tissues or platforms that physically engage antigen-presenting cells (APCs) directly [59,60]. Enhancements like gene gun or lipid nanoparticles may possibly result in sufficient antigen expression levels to trigger robust primary T-cell responses in the selected models.

4.2. Adjuvant Effects and Confounding Variables

The incorporation of hBD3 as an adjuvant, while biologically justified, introduced significant confounding effects that complicate the interpretation of immune responses. Human beta defensins can function as active immunological drivers rather than passive enhancers, capable of inducing dendritic cell maturation, cytokine production, and T-cell activation independent of specific antigens [61,62]. The observation that hBD3-containing constructs without epitopes induced measurable T-cell activation highlights this confounding effect.

Besides, some studies indicate that hBD3 preferentially amplifies specific innate immune pathways and responses, leading to a massive surge of innate “noise” [63]. While this makes hBD3 an attractive candidate for specific vaccines, our results suggest that such robust innate activation may have confounded our specific in vitro and in vivo models. This potent adjuvant-mediated activation may have masked weaker epitope-driven responses, creating a “signal-to-noise” problem where genuine antigen-specific immunity was obscured by background stimulation. The immune system became generally inflamed but not specifically targeted. Future experimental designs should incorporate dose–response studies of adjuvants, hBD3-only controls, and potentially alternative adjuvant strategies to decouple non-specific from antigen-specific effects.

4.3. Experimental System Limitations

Several methodological constraints limited our ability to definitively assess antigen-specific immunity:

In vitro System Constraints: The THP-1/Jurkat co-culture system was originally implemented as a New Approach Method (NAM) to simulate the interaction between lymphocytes and monocytes [47]. This system was selected to avoid the inherent variability of primary tissue cells and the ethical constraints of animal models, providing a standardized, biosafety-compliant platform. While this model offered an environment for observing cell–cell crosstalk, our findings ultimately highlighted its limitations in capturing the full complexity of antigen presentation and T-cell stimulation. PMA/ionomycin differentiation of THP-1 cells was necessary to provide macrophage-like function for the expression of the essential machinery for antigen presentation and co-stimulation. This phenotype possibly induced a strong background activation that was largely antigen-independent. This high baseline activation made it extremely difficult to discern subtle antigen-specific responses, potentially masking biologically relevant but modest epitope-driven immunity.

Control Limitations: A critical limitation of this study was the absence of an irrelevant antigen control, a construct delivering unrelated peptides via an identical vector backbone and adjuvant system. Without such controls, we cannot definitively attribute observed viral load reductions to epitope-specific immunity versus non-specific platform effects. This represents a significant interpretive constraint that should be addressed in future studies through the inclusion of well-matched negative controls.

Statistical Power and Study Design: The BALB/c cohorts (n = 2 per group) were underpowered for formal statistical analysis and should be interpreted as exploratory pilot data only. The limited 7-day monitoring period in IFNAR$^{-/-}$ mice may have been insufficient to capture delayed protective responses or immune memory formation. Future studies should incorporate longer observation periods and larger group sizes where feasible.

4.4. Viral Load Reduction Without Survival Benefit

The observation that several peptide groups achieved significant 2–3 log reductions in tissue viral RNA and infectious titers without corresponding survival benefit requires mechanistic interpretation. This dissociation suggests that while some immune activity was induced, it was insufficient to control systemic infection or prevent fatal outcomes. Several explanations are possible:

(i) ***Temporal mismatch:*** The immune responses may have been too slow to prevent rapid viral dissemination in the highly susceptible IFNAR$^{-/-}$ model; (ii) ***Organ-specific effects:*** Viral load reductions in spleen and liver may not reflect protection at other critical sites such as the central nervous system; (iii) ***Threshold effects:*** Protective immunity may require log-fold greater reductions than observed; (iv) ***Immune correlates:*** Survival may depend on specific immune effector mechanisms (e.g., CD8+ T-cell cytotoxicity, neutralizing antibodies) that were not adequately induced by our constructs.

The unexpected finding of higher viral titers in the full-length NP group compared to sham controls also warrants particular attention. Potential explanations include: (i) inefficient expression or presentation of the full-length protein compared to shorter epitope constructs; (ii) induction of regulatory responses that dampened antiviral immunity; (iii) sampling variability due to rapid disease progression in some animals; or (iv) possible immunopathological effects of NP-specific responses that enhanced viral replication or tissue damage.

4.5. Nucleoprotein as a Vaccine Target: Lessons Learned

Our findings contribute to the growing body of literature on NP-based CCHFV vaccine development, while highlighting both the promise and limitations of this approach. For CCHFV, the glycoprotein complex (Gn/Gc) represents the primary target for neutralizing immunity and has been successfully used in several vaccine platforms [64]. However,

envelope proteins often exhibit higher variability than internal proteins, potentially limiting cross-strain protection. CCHFV glycoproteins show low-to-moderate conservation across genotypes, but significant antigenic variation exists. In contrast, the nucleoprotein demonstrates exceptional conservation across circulating strains. Our findings suggest that NP-based vaccines may require combination approaches: (i) heterologous prime-boost strategies using different delivery platforms; (ii) combination with envelope protein targets to induce both cellular and neutralizing immunity; or (iii) enhanced delivery systems that can overcome the inherently lower immunogenicity of internal viral proteins.

4.6. Immunoinformatics Pipeline: Strengths and Limitations

The computational component of this study demonstrates both the potential and current limitations of immunoinformatics-guided vaccine design. Our systematic approach, integrating multiple prediction algorithms with comprehensive safety and population coverage analyses, represents current best practices in the field. However, several aspects warrant critical evaluation:

Threshold Optimization: The decision to lower the VaxiJen antigenicity threshold from 0.4 to 0.3025 to match the full-length NP score represents a methodological compromise that may have inflated the epitope number. While this approach was intended to maintain biological relevance, it potentially reduced prediction specificity. Future studies should employ multiple complementary antigenicity prediction tools and use cross-validation approaches rather than single-tool thresholds.

Conservation* vs. *Population Coverage Trade-offs: Our prioritization of sequence conservation over HLA population coverage reflects the global distribution of CCHFV and the need for broad-spectrum vaccines. However, this approach may have inadvertently selected epitopes with limited immunogenic potential. A more nuanced approach might weigh the balance between the conservation of epitopes and their immunogenicity. Our reliance on high conservation served as a thread to navigate algorithmic variability, but it may have overlooked epitopes with higher processing efficiency. This also highlights the need for computational models to better incorporate proteasomal degradation dynamics.

Validation Gap: The substantial disconnect between computational predictions and experimental outcomes highlights ongoing challenges in immunoinformatics. Current algorithms excel at predicting MHC binding but struggle to accurately model the complex cellular processes governing T-cell priming, activation, and memory formation in vivo.

4.7. Future Directions and Methodological Recommendations

Based on our findings, several strategic directions emerge for next-generation CCHFV vaccine development:

Enhanced Delivery Platforms: (i) Electroporation-enhanced DNA vaccination to improve cellular uptake and expression; (ii) heterologous prime-boost approaches combining DNA priming with viral vector or protein boosting; (iii) nanoparticle-based delivery systems for improved antigen presentation; (iv) modified mRNA platforms that may overcome DNA vaccine immunogenicity limitations.

Improved Experimental Design: (i) Inclusion of matched irrelevant antigen controls in all studies; (ii) systematic evaluation of adjuvant effects through dose–response and mechanism-of-action studies; (iii) employment of more physiological antigen presentation systems for in vitro validation; (iv) extended monitoring periods and larger group sizes for adequate statistical power.

Refined Computational Approaches: (i) Integration of proteasomal processing and TAP transport predictions into epitope selection; (ii) machine learning approaches that incorporate experimental validation data to improve prediction accuracy; (iii) population-

specific optimization based on HLA frequencies in CCHF-endemic regions; (iv) multi-objective optimization balancing conservation, immunogenicity, and population coverage.

Alternative Target Integration: (i) Combination NP/glycoprotein vaccines to induce both cellular and neutralizing immunity; (ii) inclusion of non-structural protein targets that may provide additional T-cell epitopes; (iii) conserved region identification across multiple bunyavirus species for pan-bunyavirus vaccine development.

4.8. Broader Implications for Computational Vaccinology

This study contributes to ongoing discussions about the maturity and limitations of computational vaccine design approaches. While immunoinformatics tools have advanced significantly, our findings underscore that effective epitope prediction does not guarantee immunological success. The field must advance from purely computational approaches toward integrated experimental-computational frameworks that incorporate:

Iterative Design Cycles: Rather than single-pass computational design followed by experimental validation, successful vaccine development may require multiple rounds of design-test-redesign with computational models updated based on experimental feedback.

Systems Immunology Integration: Future approaches should incorporate broader systems-level understanding of immune responses, including innate immunity, immune cell trafficking, and immunological memory formation.

Negative Data Integration: The field must better capture and utilize negative experimental results, such as those presented here, to improve computational models and prevent repetition of unsuccessful approaches.

5. Conclusions

This study combined in silico epitope prioritization with systematic in vitro and in vivo evaluations to assess multiepitope DNA vaccine constructs against CCHFV. The core findings demonstrate significant challenges in translating computational epitope predictions into effective vaccines: (i) In vitro assays revealed predominantly antigen-independent T-cell activation without clear evidence of epitope-specific immune responses; (ii) BALB/c mice (exploratory cohorts) showed no CCHFV-specific IgG seroconversion and only weak cytokine responses; and (iii) while several peptide constructs achieved significant reductions in tissue viral RNA and infectious titers in IFNAR$^{-/-}$ mice, these effects did not translate into survival benefit.

Rather than representing a failed vaccine attempt, these results provide essential benchmark data that highlight critical gaps between computational promise and biological reality. The systematic experimental framework presented here, linking immunoinformatics prediction through in vitro validation to in vivo efficacy testing, offers a replicable template for evaluating epitope-based vaccines against CCHFV and other high-containment pathogens.

Key methodological insights include: (i) epitope selection strategies should incorporate proteasomal cleavage modeling (ii) the necessity for appropriate control groups, particularly irrelevant antigen controls, in vaccine studies; (iii) the importance of understanding adjuvant-mediated confounding effects; (iv) the challenges of detecting antigen-specific responses in high-background experimental systems; and (v) the need for enhanced delivery platforms to achieve DNA vaccine immunogenicity.

These findings inform future vaccine redesign strategies by identifying specific areas requiring optimization: epitope selection methodologies, construct architecture, delivery platform enhancement, and experimental validation approaches. The work thus serves as a foundational framework for rational development and optimization of next-generation epitope-based vaccines against CCHF, emphasizing the critical importance of rigorous experimental validation in computational vaccinology.

Supplementary Materials: The following supporting information can be downloaded at: https://www.mdpi.com/article/10.3390/applbiosci5020025/s1, Supplementary File S1: Sequence of Ank-2 strain; Table S1: Protein sequences from other *Orthonairovirus haemorrhagiae* strains; Table S2: Prediction of MHC-I epitopes with binding affinity to CCHFV-NP using the IEDB database (August 2020 data); Table S3: Prediction of MHC-I epitopes with binding affinity to CCHFV-NP using the NetMHC 4.0 database (August 2020 data); Table S4: Prediction of MHC-I epitopes with binding affinity to CCHFV-NP using the Rankpep database (August 2020 data); Table S5: VaxiJen antigenicity scores of predicted MHC-I peptides; Table S6: The online immunoinformatics tools VaxiJen and Prediction of Anti-Inflammatory Peptides, the antigenicity scores of CCHF-NP MHC-I epitopes; Table S7: Allergenicity analysis of selected epitopes; Table S8: Toxicity analysis of selected epitopes; Table S9: Hydrophobicity analysis of selected epitopes; Table S10: Population coverage analysis of selected peptides (IEDB); Table S11: Properties of the ultimately selected CTL epitopes; Table S12: Overview of the immunoinformatics pipeline and selection logic; Table S13: Ct values for CCHFV in spleen and liver by experimental groups; Table S14: Ct values for GAPDH in spleen and liver by experimental groups; Supplementary Figure S1: Global population coverage values of the peptides; Supplementary Figure S2: Western blotting of recombinant CCHFV-NP to evaluate IgG responses by ELISA, 54 kDa; Supplementary Figure S3: Representative amplification and standard curves qPCRs.

Author Contributions: S.A.: Conceptualization (equal); data curation (lead); formal analysis (lead); investigation (lead); methodology (equal); project administration (lead); visualization (lead); writing—original draft (lead). M.E.: Conceptualization (equal); funding acquisition (lead); methodology (equal); resources (support); supervision (support); validation (support), writing—review and editing (equal). A.O.: Conceptualization (equal); funding acquisition (lead); methodology (equal); resources (support); supervision (support); validation (support); software (lead); writing—original draft (support); writing—review and editing (lead). All authors have read and agreed to the published version of the manuscript.

Funding: This study was financially supported by the Scientific and Technological Research Council of Turkey (TÜBİTAK, project #121S289) and Ankara University Scientific Research Projects (project #TDK-2022-2308).

Institutional Review Board Statement: The animal study protocol was approved by the Local Ethics Committee for Animal Experiments of Ankara University (18.03.2020/2020-6-54).” for studies involving animals.

Informed Consent Statement: Not applicable.

Data Availability Statement: The original contributions presented in this study are included in the article and Supplementary Materials. Further inquiries can be directed to the corresponding authors.

Acknowledgments: The authors gratefully acknowledge the Scientific and Technological Research Council of Turkiye (TÜBİTAK) and Ankara University for their financial support of this research.

Conflicts of Interest: The authors declare no conflicts of interest. The funders had no role in the design of the study; in the collection, analyses, or interpretation of data; in the writing of the manuscript; or in the decision to publish the results.

Abbreviations

The following abbreviations are used in this manuscript:

Crimean-Congo Hemorrhagic Fever	CCHF
Nucleoprotein	NP
Crimean-Congo Hemorrhagic Fever Virus	CCHFV
Cytotoxic T lymphocyte	CTL
human beta defensin-3	hBD3
Glycoprotein PreCursor	GPC

Immune epitope database's	IEDB
Major Histocompatibility Complex Class-I	MHC-I
Human leukocyte antigens	HLA
Full-length	FL
Human Cytomegalovirus	hCMV
Porcine teschovirus-1 2A	p2A
Alanine-alanine-tyrosine	AAY
Lentiviral vectors	LV
Seamless Ligation Cloning Extract	SLiCE
Phorbol 12-myristate-13-acetate	PMA
PolyEthylenImine	PEI
Immunoglobulin G	IgG
Phosphate-buffered saline	PBS
Horseradish peroxidase	HRP
Enzyme-linked immunosorbent assay	ELISA
Multiplicity of infection	MOI
Interferon gamma	IFN-γ
Interleukin 2	IL-2
Tumor necrosis factor alpha	TNF-α
Interleukin 6	IL-6
Interleukin 4	IL-4
Interleukin 10	IL-10
Interleukin 5	IL-5
Interleukin 13	IL-13
Nuclear factor kappa-light-chain-enhancer of activated B cells	NF-κB

References

1. Arslan, M. Evaluation of epidemiological, clinical, laboratory and treatment characteristics of Crimean-Congo hemorrhagic fever patients: Results of a 10-year analysis. *North. Clin. Istanb.* **2024**, *11*, 177–183. [CrossRef]
2. Frank, M.G.; Weaver, G.; Raabe, V. State of the Clinical Science Working Group of the National Emerging Pathogens Training and Education Center's Special Pathogens Research Network. Crimean-Congo hemorrhagic fever virus for clinicians: Virology, pathogenesis, and pathology. *Emerg. Infect. Dis.* **2024**, *30*, 847–853. [CrossRef] [PubMed]
3. Karanam, S.K.; Nagvishnu, K.; Uppala, P.K.; Edhi, S.; Varri, S.R. Crimean-Congo hemorrhagic fever: Pathogenesis, transmission and public health challenges. *World J. Virol.* **2025**, *14*, 100003. [CrossRef] [PubMed]
4. Sorvillo, T.E.; Rodriguez, S.E.; Hudson, P.; Carey, M.; Rodriguez, L.L.; Spiropoulou, C.F.; Bird, B.H.; Spengler, J.R.; Bente, D.A. Toward a sustainable One Health approach to Crimean-Congo hemorrhagic fever prevention: Focus areas and gaps in knowledge. *Trop. Med. Infect. Dis.* **2020**, *5*, 113. [CrossRef] [PubMed]
5. Khwarahm, N.R. Predicting the spatial distribution of *Hyalomma* ssp., vector ticks of Crimean-Congo hemorrhagic fever in Iraq. *Sustainability* **2023**, *15*, 13669. [CrossRef]
6. Bonnet, S.I.; Vourc'h, G.; Raffetin, A.; Falchi, A.; Figoni, J.; Fite, J.; Hoch, T.; Moutailler, S.; Quillery, E. The control of *Hyalomma* ticks, vectors of the Crimean-Congo hemorrhagic fever virus: Where are we now and where are we going? *PLoS Negl. Trop. Dis.* **2022**, *16*, e0010846. [CrossRef]
7. Eslava, M.; Carlos, S.; Reina, G. Crimean-Congo hemorrhagic fever virus: An emerging threat in Europe with a focus on epidemiology in Spain. *Pathogens* **2024**, *13*, 770. [CrossRef]
8. Norman, F.F.; Arce, O.A.; Díaz-Menéndez, M.; Belhassen-García, M.; González-Sanz, M. Changes in the epidemiology of Crimean-Congo hemorrhagic fever: Impact of travel and a One Health approach in the European region. *Travel. Med. Infect. Dis.* **2025**, *64*, 102806. [CrossRef]
9. Semper, A.E.; Olver, J.; Warner, J.; Cehovin, A.; Fay, P.C.; Hart, P.J.; Golding, J.P.; Benassi, V.; Preziosi, M.P.; Al-Asadi, K.H.R.; et al. Research and product development for Crimean-Congo hemorrhagic fever: Priorities for 2024–2030. *Lancet Infect. Dis.* **2025**, *25*, e223–e234. [CrossRef]
10. Soares-Weiser, K.; Thomas, S.; Garner, P. Ribavirin for Crimean-Congo hemorrhagic fever: Systematic review and meta-analysis. *BMC Infect. Dis.* **2010**, *10*, 207. [CrossRef]

11. D'Addiego, J.; Elaldi, N.; Wand, N.; Osman, K.; Bagci, B.K.; Kennedy, E.; Pektas, A.N.; Hart, E.; Slack, G.; Hewson, R. Investigating the effect of ribavirin treatment on genetic mutations in Crimean-Congo hemorrhagic fever virus through next-generation sequencing. *J. Med. Virol.* **2023**, *95*, e28548. [CrossRef] [PubMed]
12. Behboudi, E.; Kakavandi, E.; Hamidi-Sofiani, V.; Ebrahimian, A.; Shayestehpour, M. Crimean-Congo hemorrhagic fever virus vaccine: Past, present, and future. *Rev. Res. Med. Microbiol.* **2022**, *33*, 109–117. [CrossRef]
13. Pollard, A.J.; Bijker, E.M. A guide to vaccinology: From basic principles to new developments. *Nat. Rev. Immunol.* **2021**, *21*, 83–100. [CrossRef] [PubMed]
14. Nosrati, M.; Behbahani, M.; Mohabatkar, H. Toward the first multiepitope recombinant vaccine against Crimean-Congo hemorrhagic fever virus: A computer-aided vaccine design approach. *J. Biomed. Inf.* **2019**, *93*, 103160. [CrossRef]
15. Mortazavi, B.; Molaei, A.; Fard, N.A. Multiepitope vaccines, from design to expression: An in silico approach. *Hum. Immunol.* **2024**, *85*, 110804. [CrossRef]
16. Alizadeh, M.; Amini-Khoei, H.; Tahmasebian, S.; Ghatrehsamani, M.; Ghatreh Samani, K.; Edalatpanah, Y.; Rostampur, S.; Salehi, M.; Ghasemi-Dehnoo, M.; Azadegan-Dehkordi, F.; et al. Designing a novel multi-epitope vaccine against Ebola virus using reverse vaccinology approach. *Sci. Rep.* **2022**, *12*, 7757. [CrossRef]
17. Ahmad, S.; Demneh, F.M.; Rehman, B.; Almanaa, T.N.; Akhtar, N.; Pazoki-Toroudi, H.; Shojaeian, A.; Ghatrehsamani, M.; Sanami, S. In silico design of a novel multi-epitope vaccine against HCV infection through immunoinformatics approaches. *Int. J. Biol. Macromol.* **2024**, *267*, 131517. [CrossRef]
18. Ullah, H.; Ullah, S.; Li, J.; Yang, F.; Tan, L. An in silico design of a vaccine against all serotypes of the dengue virus based on virtual screening of B-cell and T-cell epitopes. *Biology* **2024**, *13*, 681. [CrossRef]
19. Ghattas, M.; Dwivedi, G.; Lavertu, M.; Alameh, M.-G. Vaccine technologies and platforms for infectious diseases: Current progress, challenges, and opportunities. *Vaccines* **2021**, *9*, 1490. [CrossRef]
20. Sunita; Sajid, A.; Singh, Y.; Shukla, P. Computational tools for modern vaccine development. *Hum. Vaccin. Immunother.* **2019**, *16*, 723–735. [CrossRef]
21. Kozak, M.; Hu, J. DNA vaccines: Their formulations, engineering and delivery. *Vaccines* **2024**, *12*, 71. [CrossRef]
22. Karaaslan, E.; Çetin, N.S.; Kalkan-Yazıcı, M.; Hasanoğlu, S.; Karakeçili, F.; Özdarendeli, A.; Kalkan, A.; Kılıç, A.O.; Doymaz, M.Z. Immune responses in multiple hosts to nucleocapsid protein (NP) of Crimean-Congo hemorrhagic fever virus (CCHFV). *PLoS Negl. Trop. Dis.* **2021**, *15*, e0009973. [CrossRef]
23. Scholte, F.E.M.; Karaaslan, E.; O'Neal, T.J.; Sorvillo, T.E.; Genzer, S.C.; Welch, S.R.; Kainulainen, M.H.; Montgomery, J.M.; Pegan, S.D. Vaccination with the Crimean-Congo hemorrhagic fever virus viral replicon vaccine induces NP-based T-cell activation and antibodies possessing Fc-mediated effector functions. *Front. Cell Infect. Microbiol.* **2023**, *13*, 1233148. [CrossRef] [PubMed]
24. Goedhals, D.; Paweska, J.T.; Burt, F.J. Long-lived CD8+ T-cell responses following Crimean-Congo hemorrhagic fever virus infection. *PLoS Negl. Trop. Dis.* **2017**, *11*, e0006149. [CrossRef]
25. Pirincal, A.; Doymaz, M.Z. The role of nucleocapsid protein (NP) in the immunology of Crimean-Congo hemorrhagic fever virus (CCHFV). *Viruses* **2024**, *16*, 1547. [CrossRef]
26. Kalkan-Yazıcı, M.; Karaaslan, E.; Güler-Çetin, N.S.; Doymaz, M.Z. Cellular immunity to nucleoproteins (NP) of Crimean-Congo hemorrhagic fever virus (CCHFV) and Hazara virus (HAZV). *Med. Microbiol. Immunol.* **2024**, *213*, 20. [CrossRef]
27. Herst, C.V.; Burkholz, S.; Sidney, J.; Sette, A.; Harris, P.E.; Massey, S.; Brasel, T.; Cunha-Neto, E.; Rosa, D.S.; Chao, W.C.H.; et al. An effective CTL peptide vaccine for Ebola Zaire based on survivors' CD8+ targeting of a particular nucleocapsid protein epitope with potential implications for COVID-19 vaccine design. *Vaccine* **2020**, *38*, 4464–4475. [CrossRef]
28. Kupke, A.; Volz, A.; Dietzel, E.; Freudenstein, A.; Schmidt, J.; Shams-Eldin, H.; Jany, S.; Sauerhering, L.; Krähling, V.; Gellhorn Serra, M.; et al. Protective CD8+ T-cell response induced by modified vaccinia virus Ankara delivering Ebola virus nucleoprotein. *Vaccines* **2022**, *10*, 533. [CrossRef]
29. Ferris, L.K.; Mburu, Y.K.; Mathers, A.R.; Fluharty, E.R.; Larregina, A.T.; Ferris, R.L.; Falo, L.D., Jr. Human beta-defensin 3 induces maturation of human Langerhans cell-like dendritic cells: An antimicrobial peptide that functions as an endogenous adjuvant. *J. Investig. Dermatol.* **2013**, *133*, 460–468. [CrossRef] [PubMed]
30. Bharucha, J.P.; Sun, L.; Lu, W.; Gartner, S.; Garzino-Demo, A. Human beta-defensin 2 and 3 inhibit HIV-1 replication in macrophages. *Front. Cell Infect. Microbiol.* **2021**, *11*, 535352. [CrossRef] [PubMed]
31. Walewska, A.; Kosikowska-Adamus, P.; Tomczykowska, M.; Jaroszewski, B.; Prahl, A.; Bulaj, G. Improving Fmoc solid phase synthesis of human beta defensin 3. *Int. J. Mol. Sci.* **2022**, *23*, 12562. [CrossRef]
32. Trolle, T.; McMurtrey, C.P.; Sidney, J.; Bardet, W.; Osborn, S.C.; Kaever, T.; Sette, A.; Hildebrand, W.H.; Nielsen, M.; Peters, B. The length distribution of class I restricted T-cell epitopes is determined by both peptide supply and MHC allele-specific binding preference. *J. Immunol.* **2016**, *196*, 1480–1487. [CrossRef]
33. Chakraborty, S.; Deb, B.; Nath, D.; Monoswita, D. Identification of promising CD8 and CD4 T-cell epitopes for peptide vaccine formulation against SARS-CoV-2. *Arch. Microbiol.* **2022**, *204*, 242. [CrossRef] [PubMed]

34. Jiang, D.; Ma, Z.; Zhang, J.; Sun, Y.; Bai, T.; Liu, R.; Wang, Y.; Guan, L.; Fu, S.; Sun, Y.; et al. Immunoreactivity analysis of MHC-I epitopes derived from the nucleocapsid protein of SARS-CoV-2 via computation and vaccination. *Vaccines* **2024**, *12*, 1214. [CrossRef]
35. Doytchinova, I.A.; Flower, D.R. VaxiJen: A server for prediction of protective antigens, tumor antigens and subunit vaccines. *BMC Bioinform.* **2007**, *8*, 4. [CrossRef] [PubMed]
36. Kolaskar, A.S.; Tongaonkar, P.C. A semiempirical method for prediction of antigenic determinants on protein antigens. *FEBS Lett.* **1990**, *276*, 172–174. [CrossRef] [PubMed]
37. Sharma, N.; Patiyal, S.; Dhall, A.; Pande, A.; Arora, C.; Raghava, G.P.S. AlgPred 2.0: An improved method for predicting allergenic proteins and mapping of IgE epitopes. *Brief. Bioinform.* **2021**, *22*, bbaa294. [CrossRef]
38. Dimitrov, I.; Flower, D.R.; Doytchinova, I. AllerTOP: A server for in silico prediction of allergens. *BMC Bioinform.* **2013**, *14*, S4. [CrossRef]
39. Dimitrov, I.; Bangov, I.; Flower, D.R.; Doytchinova, I. AllerTOP v.2—A server for *in silico* prediction of allergens. *J. Mol. Model.* **2014**, *20*, 2278. [CrossRef]
40. Nguyen, M.N.; Krutz, N.L.; Limviphuvadh, V.; Lopata, A.L.; Gerberick, G.F.; Maurer-Stroh, S. AllerCatPro 2.0: A web server for predicting protein allergenicity potential. *Nucleic Acids Res.* **2022**, *50*, W36–W43. [CrossRef]
41. Sharma, N.; Naorem, L.D.; Jain, S.; Raghava, G.P.S. ToxinPred2: An improved method for predicting toxicity of proteins. *Brief. Bioinform.* **2022**, *23*, bbac174. [CrossRef]
42. Wei, L.; Ye, X.; Sakurai, T.; Mu, Z.; Wei, L. ToxIBTL: Prediction of peptide toxicity based on information bottleneck and transfer learning. *Bioinformatics* **2022**, *38*, 1514–1524. [CrossRef]
43. Morozov, V.; Rodrigues, C.H.M.; Ascher, D.B. CSM-Toxin: A web-server for predicting protein toxicity. *Pharmaceutics* **2023**, *15*, 431. [CrossRef]
44. Shah, M.; Rafiq, S.; Woo, H.G. Challenges and considerations in multi-epitope vaccine design surrounding toll-like receptors. *Trends Pharmacol. Sci.* **2024**, *45*, 1104–1118. [CrossRef]
45. Kim, J.H.; Lee, S.R.; Li, L.H.; Park, H.J.; Park, J.H.; Lee, K.Y.; Kim, M.K.; Shin, B.A.; Choi, S.Y. High cleavage efficiency of a 2A peptide derived from porcine teschovirus-1 in human cell lines, zebrafish and mice. *PLoS ONE* **2011**, *6*, e18556. [CrossRef]
46. Daigneault, M.; Preston, J.A.; Marriott, H.M.; Whyte, M.K.; Dockrell, D.H. The identification of markers of macrophage differentiation in PMA-stimulated THP-1 cells and monocyte-derived macrophages. *PLoS ONE* **2010**, *5*, e8668. [CrossRef]
47. Franko, N.; Sollner Dolenc, M. Evaluation of THP-1 and Jurkat cell lines coculture for the in vitro assessment of the effects of immunosuppressive substances. *Toxics* **2024**, *12*, 607. [CrossRef] [PubMed]
48. Reed, L.J.; Muench, H. A simple method of estimating fifty percent endpoints. *Am. J. Hyg.* **1938**, *27*, 493–497. [CrossRef]
49. Galloway, S.A.; Dolton, G.; Attaf, M.; Wall, A.; Fuller, A.; Rius, C.; Bianchi, V.; Theaker, S.; Lloyd, A.; Caillaud, M.E.; et al. Peptide super-agonist enhances T-cell responses to melanoma. *Front. Immunol.* **2019**, *10*, 319. [CrossRef]
50. Chylinski, K.; Hubmann, M.; Hanna, R.E.; Yanchus, C.; Michlits, G.; Uijttewaal, E.C.; Doench, J.; Schramek, D.; Elling, U. CRISPR-Switch regulates sgRNA activity by Cre recombination for sequential editing of two loci. *Nat. Commun.* **2019**, *10*, 5454. [CrossRef] [PubMed]
51. Oluka, G.K.; Namubiru, P.; Kato, L.; Ankunda, V.; Gombe, B.; Cotten, M.; COVID-19 Immunoprofiling Team; Musenero, M.; Kaleebu, P.; Fox, J.; et al. Optimization and validation of a conventional ELISA acnd cut-offs for detecting and quantifying anti-SARS-CoV-2 spike, RBD, and nucleoprotein IgG, IgM, and IgA antibodies in Uganda. *Front. Immunol.* **2023**, *14*, 1113194. [CrossRef]
52. Wang, S.; Li, W.; Wang, Z.; Yang, W.; Li, E.; Xia, X.; Yan, F.; Chiu, S. Emerging and reemerging infectious diseases: Global trends and new strategies for their prevention and control. *Signal Transduct. Target. Ther.* **2024**, *9*, 223. [CrossRef]
53. Boccalini, S. Value of vaccinations: A fundamental public health priority to be fully evaluated. *Vaccines* **2025**, *13*, 479. [CrossRef] [PubMed]
54. Alam, R.; Samad, A.; Ahammad, F.; Nur, S.M.; Alsaiari, A.A.; Imon, R.R.; Talukder, M.E.K.; Nain, Z.; Rahman, M.M.; Mohammad, F.; et al. In silico formulation of a next-generation multiepitope vaccine for use as a prophylactic candidate against Crimean-Congo hemorrhagic fever. *BMC Med.* **2023**, *21*, 36. [CrossRef] [PubMed]
55. Majid, M.; Andleeb, S. Designing a multiepitopic vaccine against the enterotoxigenic Bacteroides fragilis based on immunoinformatics approach. *Sci. Rep.* **2019**, *9*, 19780. [CrossRef]
56. Alshiekheid, M.A.; Dou, A.M.; Algahtani, M.; Al-Megrin, W.A.I.; Alhawday, Y.A.; Alradhi, A.E.; Bukhari, K.; Alharbi, B.F.; Algefary, A.N.; Alhunayhani, B.A.; et al. Bioinformatics and immunoinformatics assisted multiepitope vaccine construct against Burkholderia anthina. *Saudi Pharm. J.* **2024**, *32*, 101917. [CrossRef]
57. Cernuto, F.; Maleki, A.; Russo, G.; Di Salvatore, V.; Pappalardo, F. In-silico epitope-based vaccines design: Progress, challenges and the road ahead. *Expert Opin. Drug Discov.* **2025**, *20*, 1701–1712. [CrossRef] [PubMed]
58. Lu, B.; Lim, J.M.; Yu, B.; Song, S.; Neeli, P.; Sobhani, N.; K, P.; Bonam, S.R.; Kurapati, R.; Zheng, J.; et al. The next-generation DNA vaccine platforms and delivery systems: Advances, challenges and prospects. *Front. Immunol.* **2024**, *15*, 1332939. [CrossRef]

59. Kim, C.G.; Lee, J.C.; Ju, D.B.; Kim, S.K.; Yun, C.H.; Cho, C.S. Enhancement of immune responses elicited by nanovaccines through a cross-presentation pathway. *Tissue Eng. Regen. Med.* **2023**, *20*, 355–370. [CrossRef]
60. Romani, N.; Flacher, V.; Tripp, C.H.; Sparber, F.; Ebner, S.; Stoitzner, P. Targeting skin dendritic cells to improve intradermal vaccination. *Intradermal Immun.* **2011**, 351. [CrossRef]
61. Mei, H.F.; Jin, X.B.; Zhu, J.Y.; Zeng, A.H.; Wu, Q.; Lu, X.M.; Li, X.B.; Shen, J. β-defensin 2 as an adjuvant promotes anti-melanoma immune responses and inhibits the growth of implanted murine melanoma in vivo. *PLoS ONE* **2012**, *7*, e31328. [CrossRef]
62. Kim, J.; Cho, B.-H.; Jang, Y.-S. Understanding the roles of host defense peptides in immune modulation: From antimicrobial action to potential as adjuvants. *J. Microbiol. Biotechnol.* **2023**, *33*, 288–298. [CrossRef] [PubMed]
63. McGlasson, S.L.; Semple, F.; MacPherson, H.; Gray, M.; Davidson, D.J.; Dorin, J.R. Human β-defensin 3 increases the TLR9-dependent response to bacterial DNA. *Eur. J. Immunol.* **2017**, *47*, 658–664. [CrossRef] [PubMed]
64. McFadden, E.; Monticelli, S.R.; Wang, A.; Ramamohan, A.R.; Batchelor, T.G.; Kuehne, A.I.; Bakken, R.R.; Tse, A.L.; Chandran, K.; Herbert, A.S.; et al. Engineering and structures of Crimean-Congo hemorrhagic fever virus glycoprotein complexes. *Cell* **2025**, *188*, 303–315. [CrossRef] [PubMed]

Disclaimer/Publisher's Note: The statements, opinions and data contained in all publications are solely those of the individual author(s) and contributor(s) and not of MDPI and/or the editor(s). MDPI and/or the editor(s) disclaim responsibility for any injury to people or property resulting from any ideas, methods, instructions or products referred to in the content.